Supporting Information

Near–infrared fluorescence probes based on disassembly–induced emission pyrene derivatives†

Yuteng Zhang,‡[a] Xiongfei,‡[a] Yang Li ,‡[b] Jingyao Mao,[a] Jian Fan*[b] and Bo Song*[a]

[a] *College of Chemistry, Chemical Engineering and Materials Science, Soochow University, Suzhou 215123, P. R. China. *Email: songbo@suda.edu.cn*

[b] *Institute of Functional Nano & Soft Materials (FUNSOM), Jiangsu Key Laboratory for Carbon-Based Functional Materials & Devices, Soochow University, Suzhou, Jiangsu 215123, China *Email: jianfan@suda.edu.cn*

‡ Yuteng Zhang and Xiongfei He *contributed equally to this article*

1. The corresponding NMR and MS spectroscopy of PYN

Compound **A:**

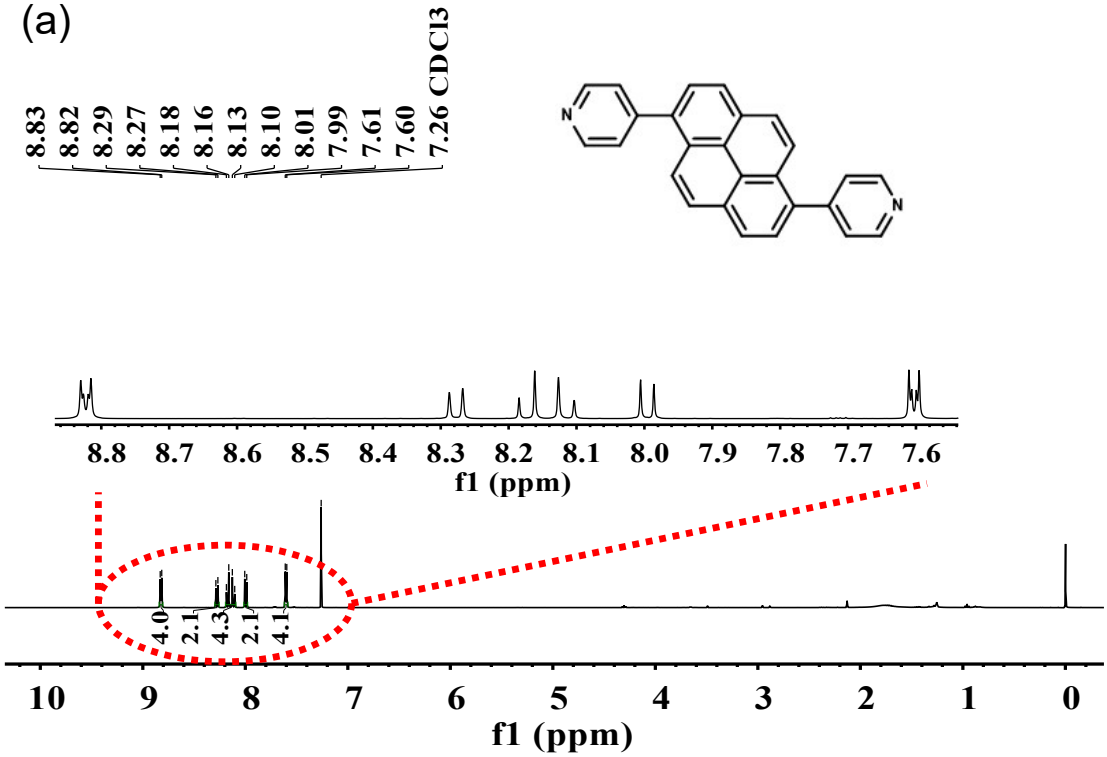
(a)
8.83
8.82
8.29
8.27
8.18
8.16
8.13
8.10
8.01
7.99
7.61
7.60
7.26 CDCl3
N
N
8.8 8.7 8.6 8.5 8.4 8.3 8.2 8.1 8.0 7.9 7.8 7.7 7.6
f1 (ppm)
4.0
2.1
4.3
2.1
4.1
10 9 8 7 6 5 4 3 2 1 0
f1 (ppm)

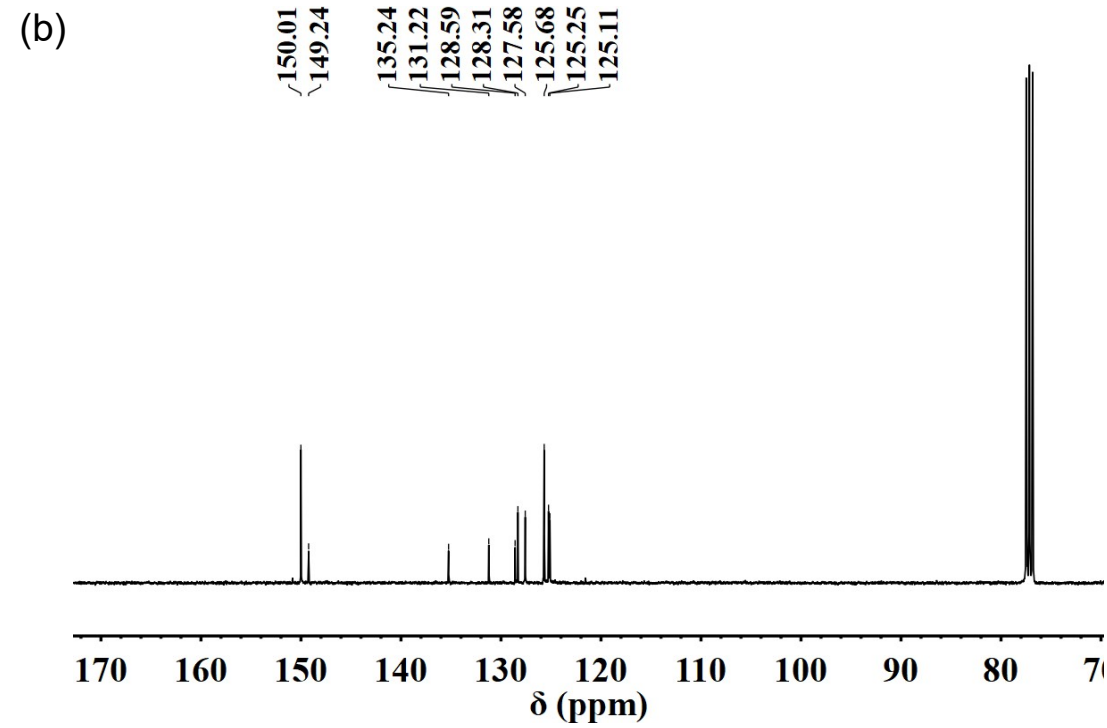
(b)
150.01
149.24
135.24
131.22
128.59
128.31
127.58
125.68
125.25
125.11
170 160 150 140 130 120 110 100 90 80
δ (ppm)

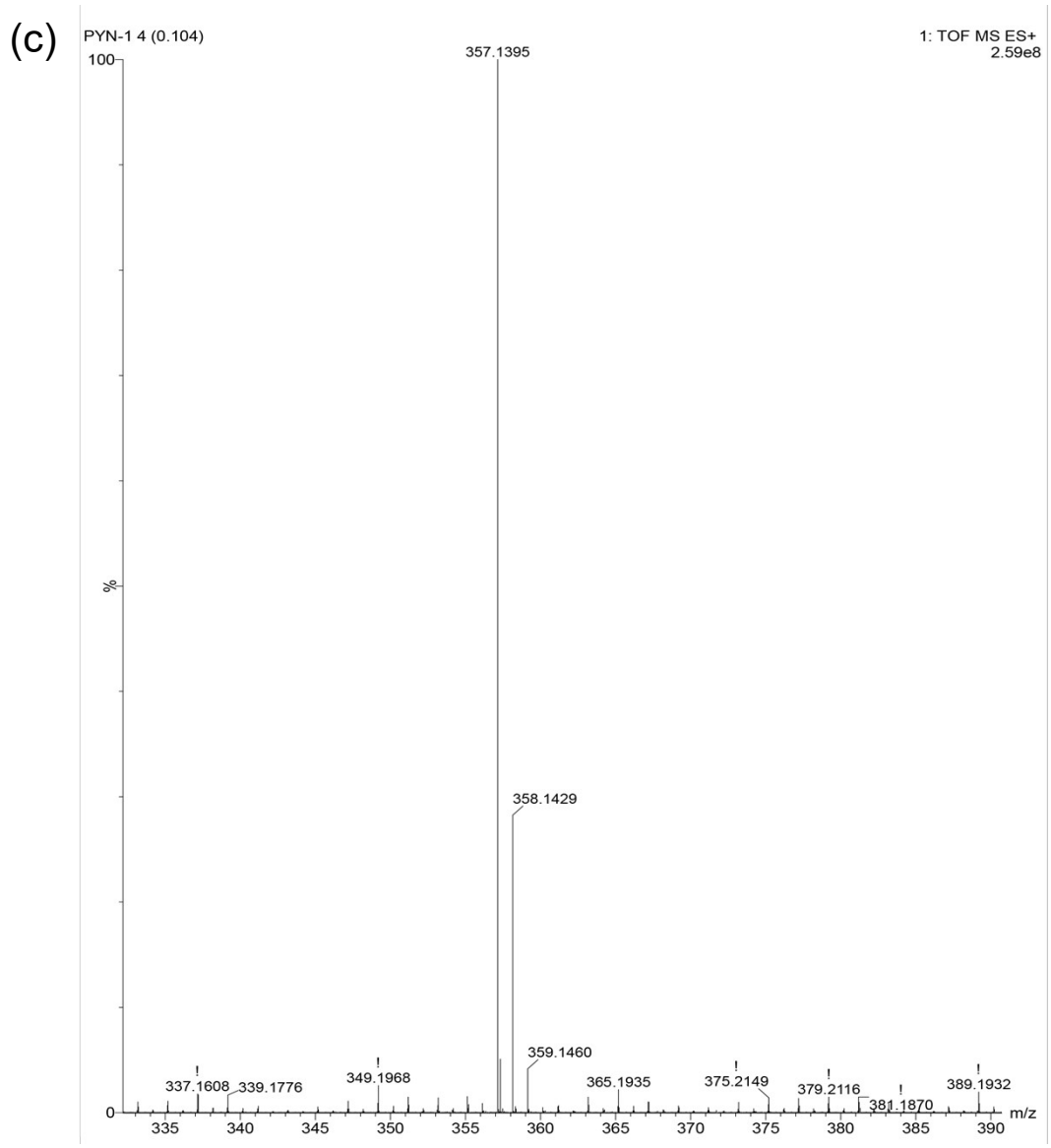

*Figure S1. (a) ^{1}H NMR spectrum of compound **A** in $CDCl_3$. (b) ^{13}C NMR spectrum of compound **A** in $CDCl_3$. (c) ESI-MS of compound **A**.*

Compound **B:**

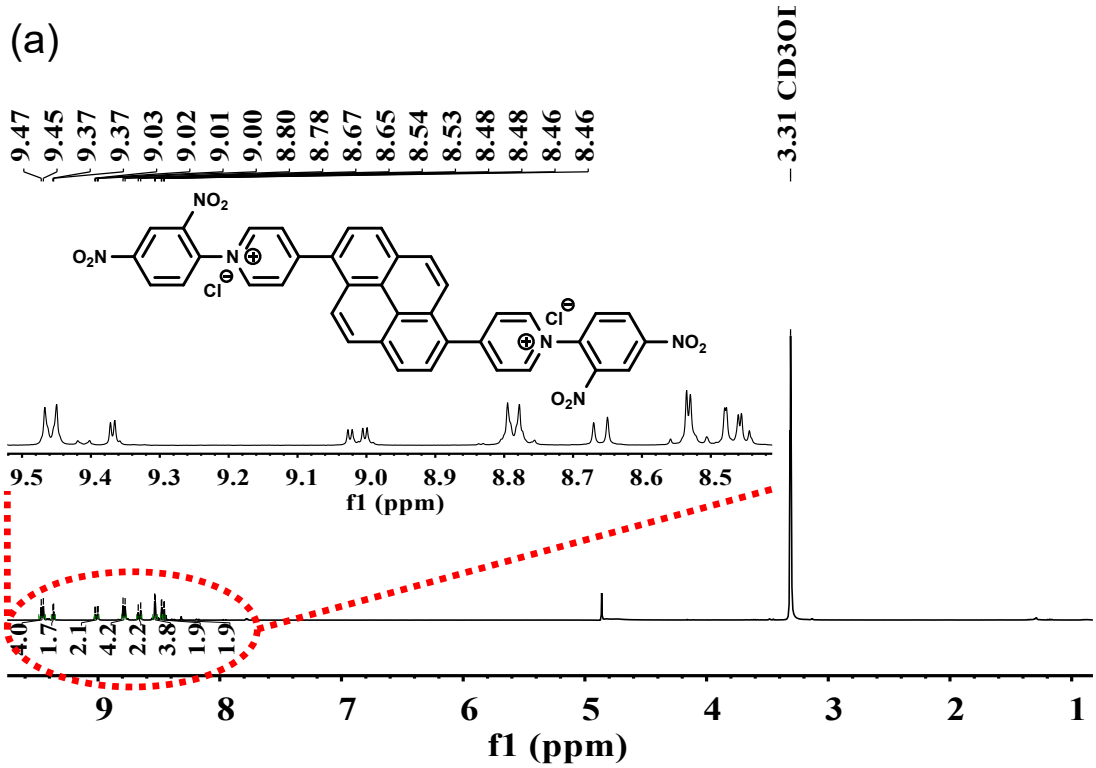
(a)
9.47
9.45
9.37
9.37
9.03
9.02
9.01
9.00
8.80
8.78
8.67
8.65
8.54
8.53
8.48
8.48
8.46
8.46
3.31 CD3OD
NO2
O2N
N
Cl
NO2
O2N
9.5 9.4 9.3 9.2 9.1 9.0 8.9 8.8 8.7 8.6 8.5
f1 (ppm)
4.0
1.7
2.1
4.2
2.2
3.8
1.9
1.9
9 8 7 6 5 4 3 2 1
f1 (ppm)

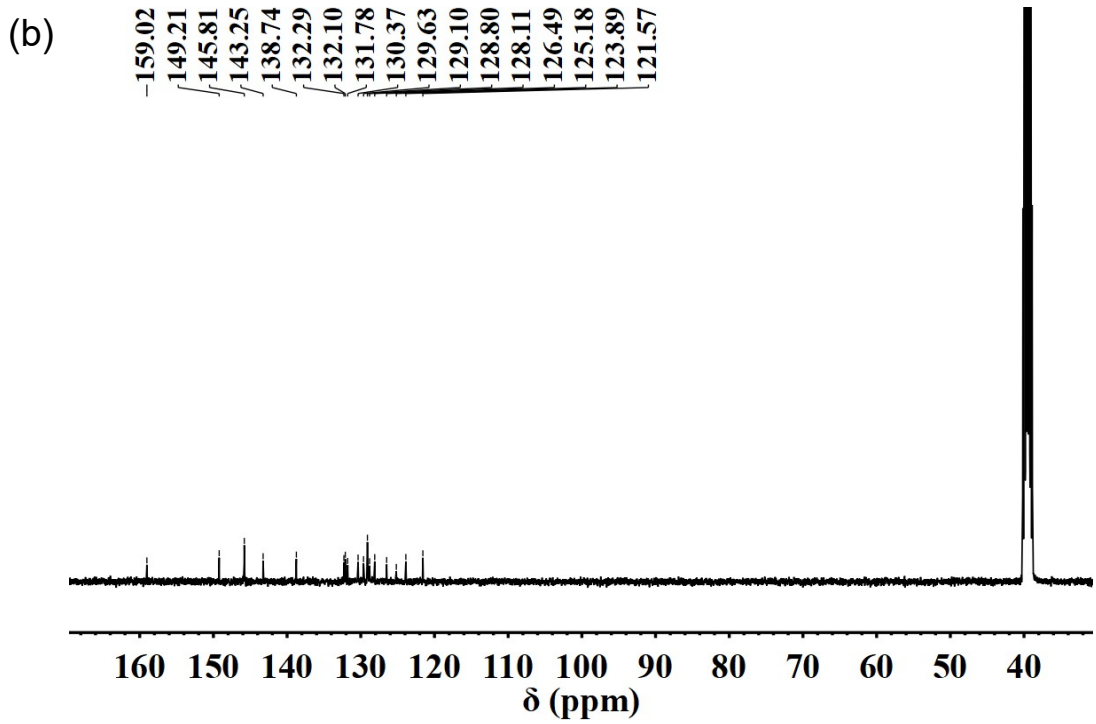
(b)
159.02
149.21
145.81
143.25
138.74
132.29
132.10
131.78
130.37
129.63
129.10
128.80
128.11
126.49
125.18
123.89
121.57
160 150 140 130 120 110 100 90 80 70 60 50 40
δ (ppm)

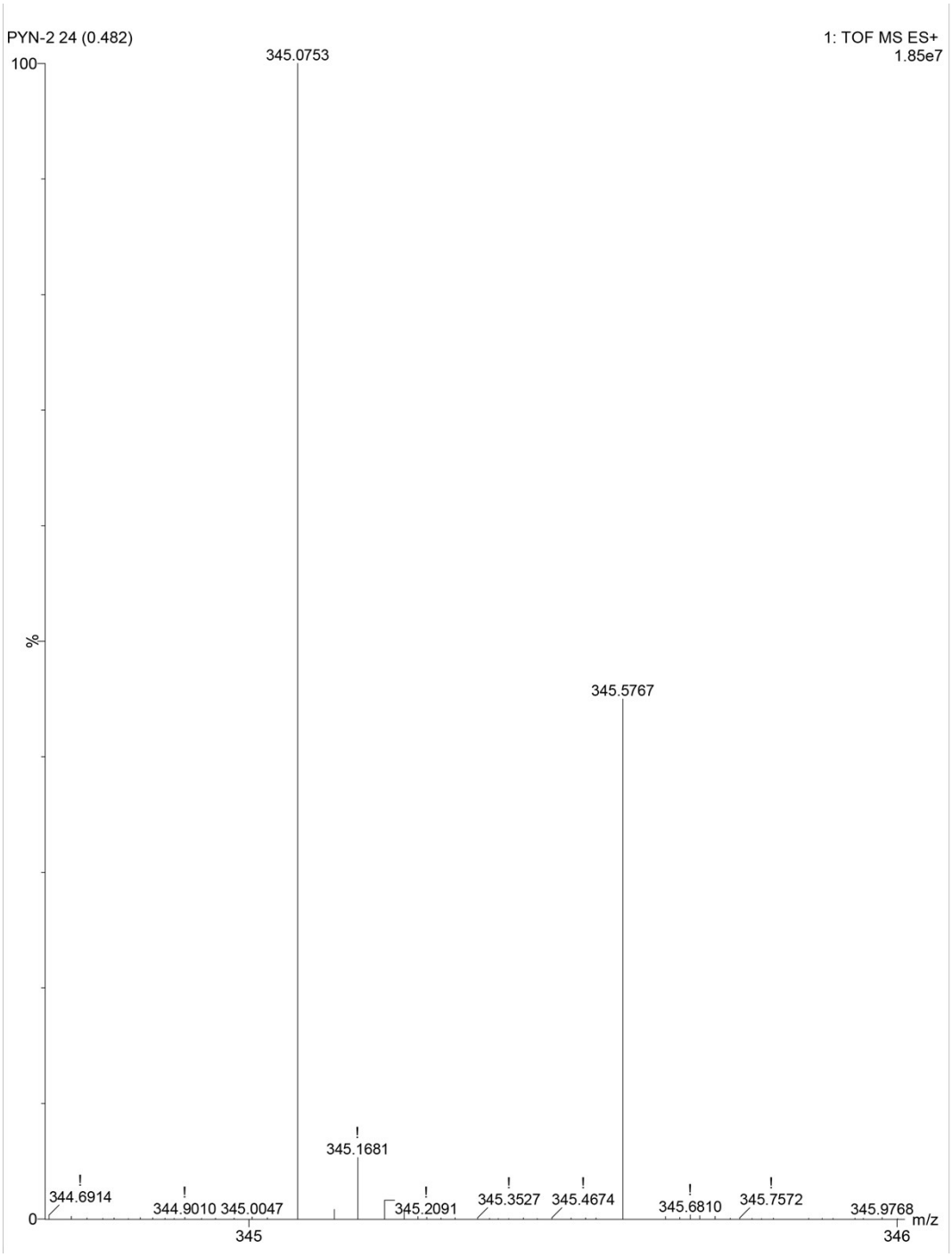

*Figure S2. (a) [1]H NMR spectrum of compound **B** in MeOD. (b) [13]C NMR spectrum of compound **B** in DMSO-d6. (c) ESI-MS of compound **B**.*

PYN**:**

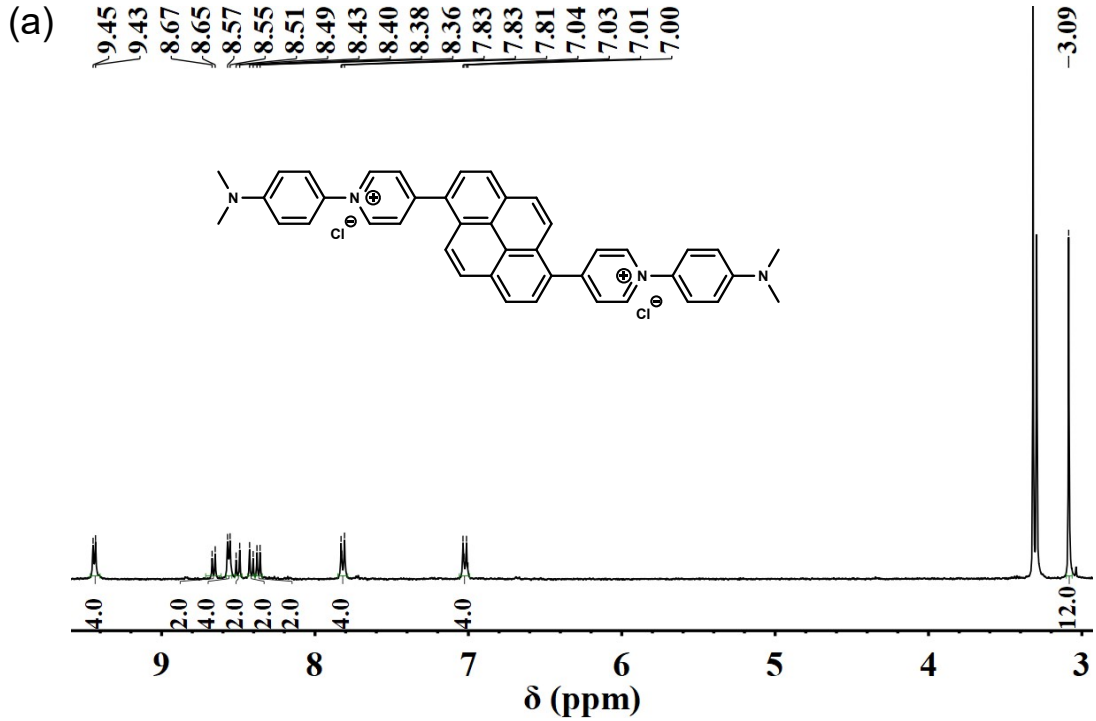
(a)
9.45
9.43
8.67
8.65
8.57
8.55
8.51
8.49
8.43
8.40
8.38
8.36
7.83
7.83
7.81
7.04
7.03
7.01
7.00
3.09
4.0
2.0
4.0
2.0
2.0
2.0
4.0
4.0
12.0
9
8
7
6
5
4
3
δ (ppm)

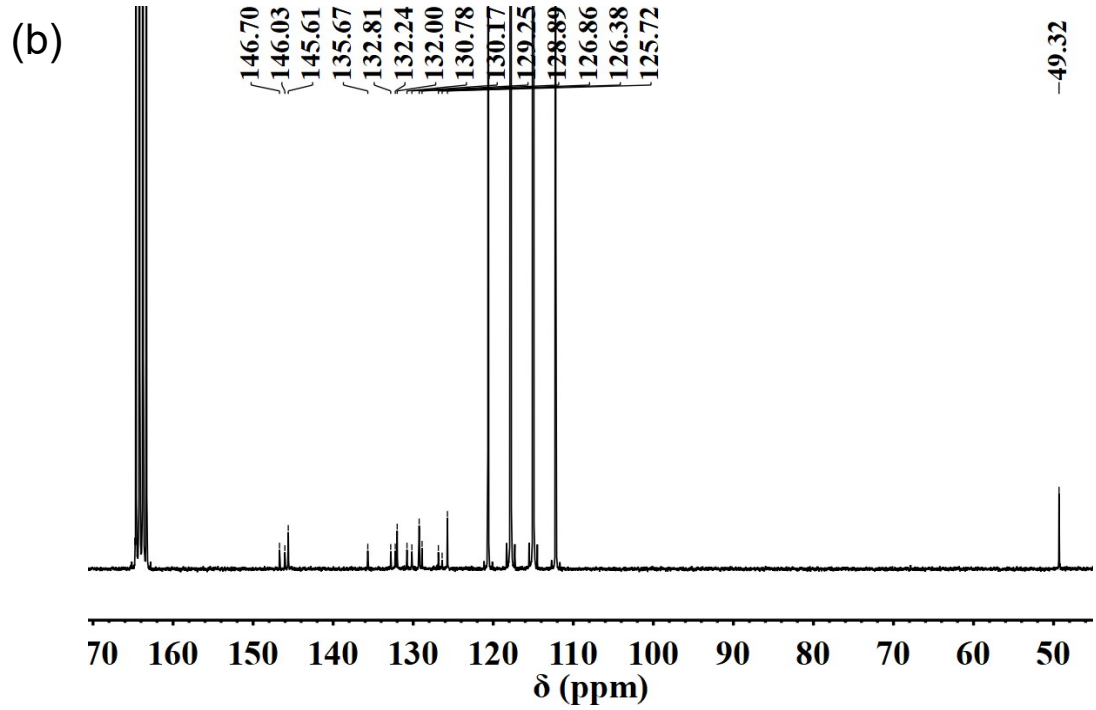
(b)
146.70
146.03
145.61
135.67
132.81
132.24
132.00
130.78
130.17
129.25
128.89
126.86
126.38
125.72
49.32
70
160
150
140
130
120
110
100
90
80
70
60
50
δ (ppm)

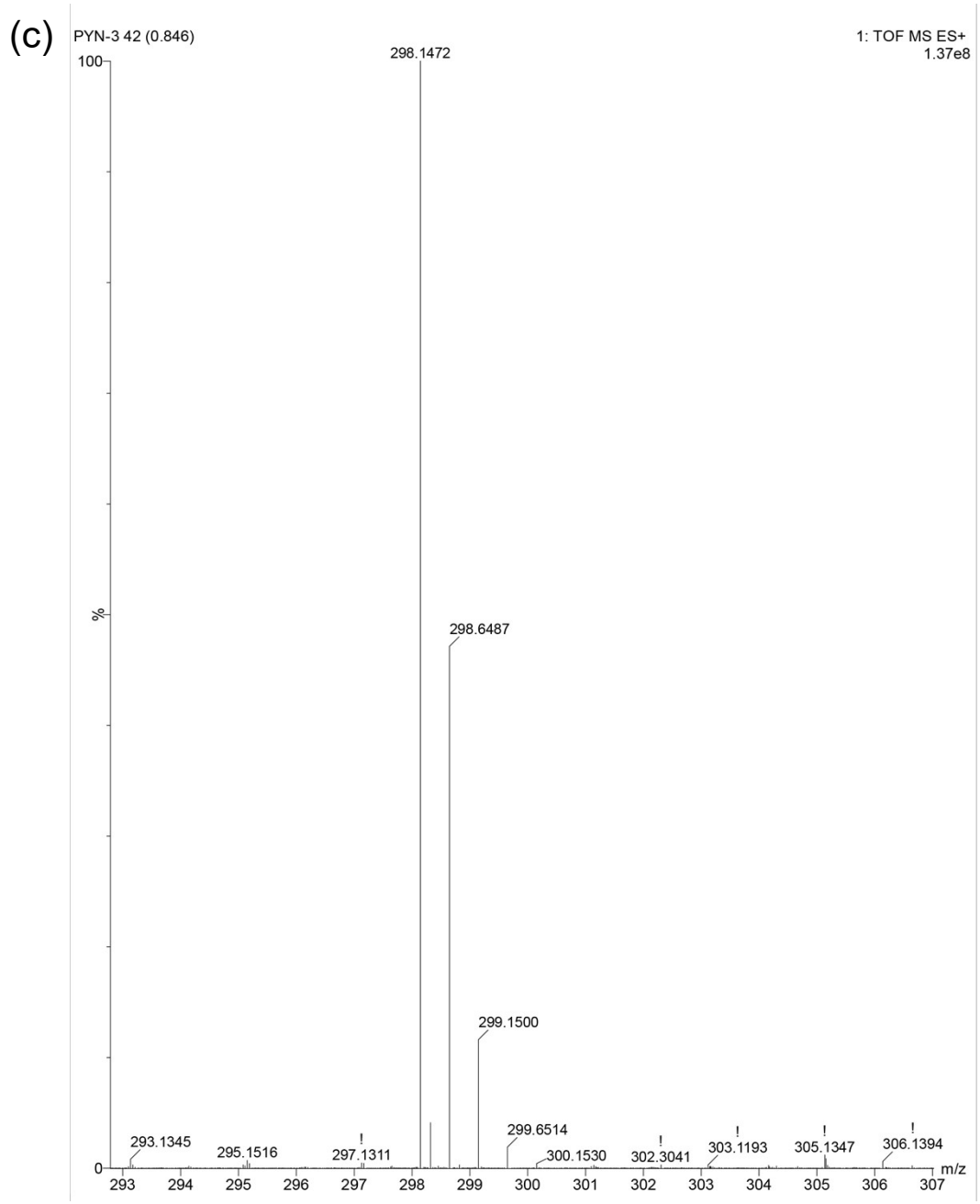

*Figure S3. (a) [1]H NMR spectrum of compound **PYN** in DMSO-d6. (b) [13]C NMR spectrum of compound **PYN** in TFA-d1. (c) ESI-MS of compound **PYN**.*

2. The solubility and the optical properties of PYN in H_2O and MeOH

The solubility of PYN in H_2O and methanol as shown in **Fig. S4 (a) and (b)**. Since PYN is an amphiphilic molecule, the solubility was assessed by the Tyndall effect. Once the light beam appears, assemblies should be formed in the solution. Using this criterion to judge the solubility, PYN has a maximum solubility of around 4-5 μmol

L^{-1}. PYN is quite soluble in MeOH; light beams appeared as the concentration reached 50-57 μmol L^{-1}.

In the aqueous solution, the aggregation of PYN resulted in the absorption peak shift from 445 to 455 nm; correspondingly, the emission peaks at 665 and 724 nm appeared, and the intensity increased with increasing the concentration of PYN.

In the methanol solution, the aggregation did not cause any peak shift in the UV-vis spectra. In contrast, the emission peak converted from 555 to 678 nm. The emission of the aggregates in the aqueous solution is different from that in methanol. These results imply that either the molecules should be packed in different ways or the aggregates have different emission mechanisms in these two solvents.

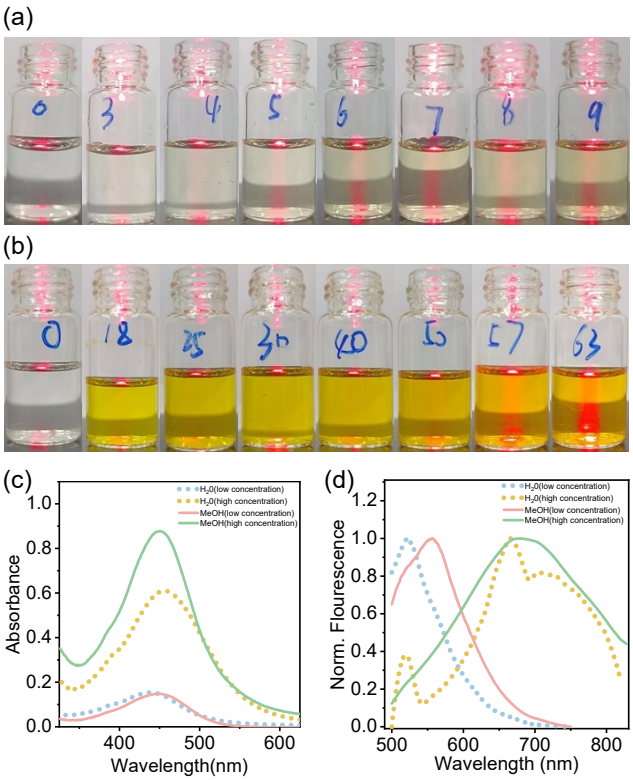

Figure S4. (a) The solubility of PYN in H_2O. (b) The solubility of PYN in MeOH. (c) The UV of PYN in H_2O and MeOH. (d) The normalised fluorescence spectra of PYN in H_2O and MeOH.

We quantified the CMC of PYN in aqueous solution by UV–vis spectroscopy. The linear fit shows a turning point at approximately 6.7×10^{-6} mol L^{-1}, corresponding to the CMC of PYN, as shown in Fig. S5.

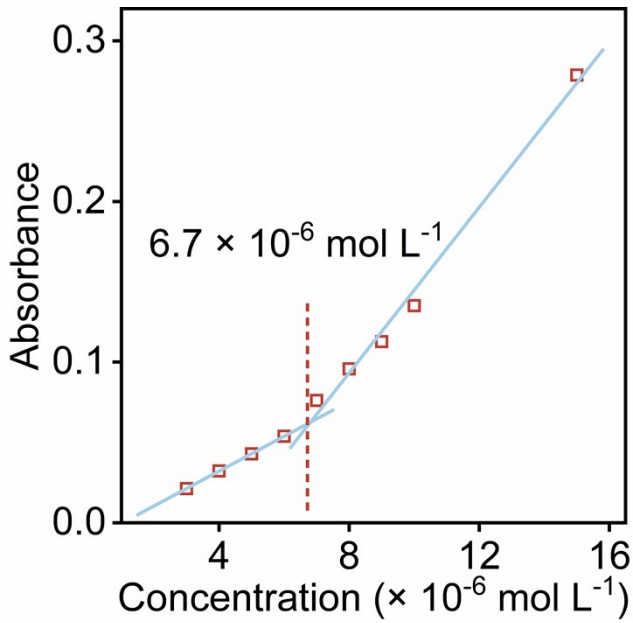

Figure S5. Absorption intensity of PYN at different concentrations.

3. The dynamics and kinetics of supramolecular binding

The kinetics of supramolecular binding by monitoring the fluorescence evolution over time. The experimental results showed that the fluorescence intensity leveled off after approximately 140 s.

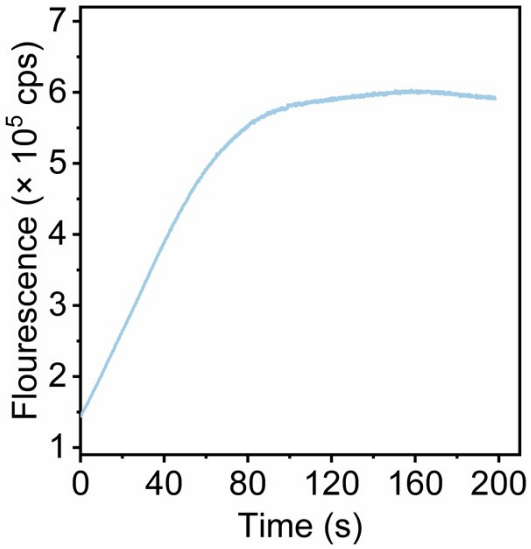

Figure S6. The fluorescence intensity at 690 nm over time after the addition of CB[8] to PYN (at RT).

The dynamics of supramolecular binding using the Benesi–Hildebrand equation. The binding ratio between PYN and CB[8] was 1:2 in aqueous solution. According to the Benesi–Hildebrand equation, we can obtain the binding constant between PYN and

CB[8]. The following equation shows the Benesi–Hildebrand equation:

$$\frac{1}{F - F_0} = \frac{1}{K_a \cdot (F_{max} - F_0) \cdot C_{CB[8]}{}^2} + \frac{1}{F_{max} - F_0} \#(1)$$

F and F_0 represent the fluorescence intensity of the solution without or after the addition of CB[8], F_{max} is the maximum fluorescence intensity of the solution after the addition of CB[8], K_a is the binding constant between PYN and CB[8], and $C_{CB[8]}$ is the concentration of the added CB[8]. As shown in **Fig. R4**, an excellent linear relationship was presented between $(F\text{-}F_0)^{-1}$ and $C_{CB[8]}{}^2$, indicating 1:2 binding between PYN and CB[8], which is consistent with previous results. In addition, the linear analytical equation obtained was $Y = 8.6 \times 10^{-17} X + 7.3 \times 10^{-8}$, in which K is the ratio of the intercept to the slope of the equation and was calculated to be 8.5×10^9 $(\text{mol L}^{-1})^{-2}$, suggesting strong binding between PYN and CB[8].

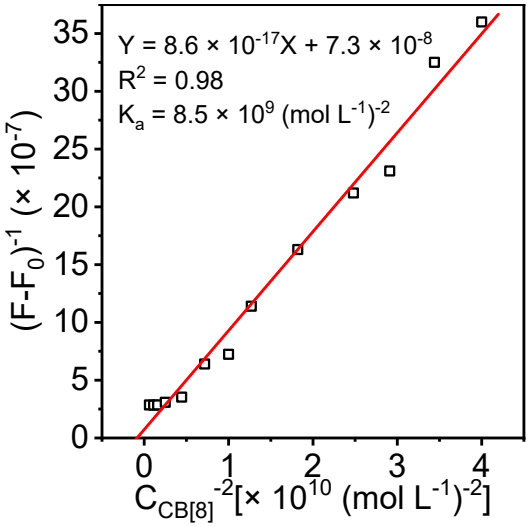

Figure S7. The Benesi-Hildebrand plots of PYN and CB[8].

4. Fluorescence quantum yield of PYN and PYN@CB[8].

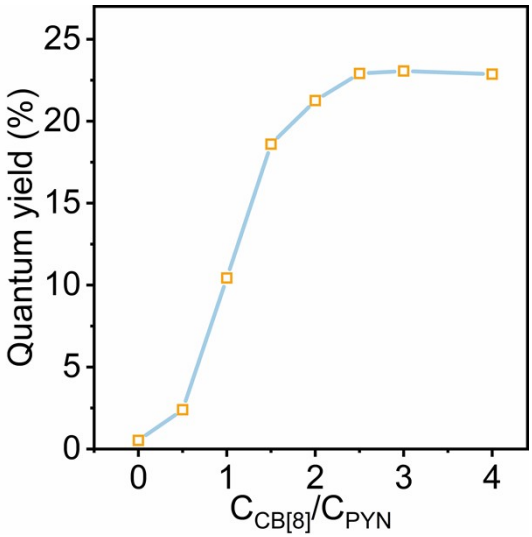

Figure S8. Fluorescence quantum yield of PYN and PYN@CB[8].

5. *Theoretical calculations of PYN@CB[8].*

Using density functional theory (DFT) and time-dependent density functional theory (TD-DFT) methods, the geometric structures of the HOMO and LUMO of PYN and PYN@CB[8] were fully optimized. The optimized structures, distributions of HOMO and LUMO and excited state levels of the lowest adiabatic excited states were analyzed by the B3LYP/6-31 g (d) basis set via the Gaussian 16 package.[1] In addition, absorption and emission spectra were obtained using the wavefunction

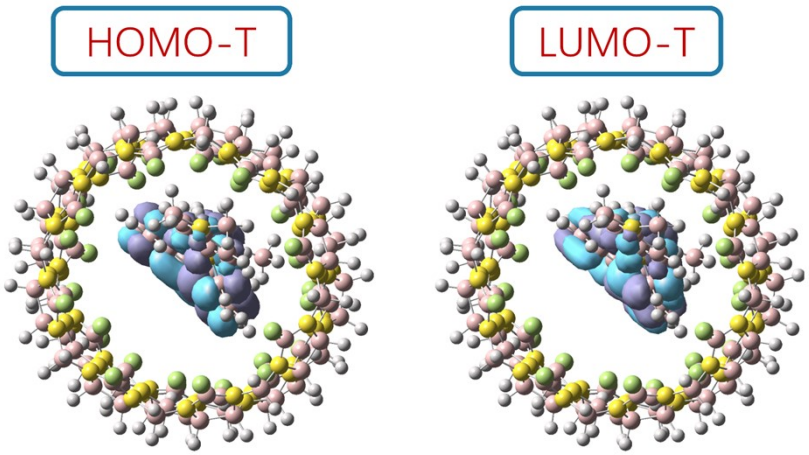

analysis software Multiwfn.[2, 3]

Figure S9. *The HOMO and LUMO distributions of PYN@CB[8](top view).*

Reference

1. M. Frisch, G. Trucks, H. Schlegel, G. Scuseria, M. Robb, J. Cheeseman, G. Scalmani, V. Barone, G. Petersson and H. Nakatsuji, *Gaussian16 (Revision A. 03)*, 2016.
2. T. Lu and Q. Chen, *Journal of Computational Chemistry*, 2022, **43**, 539-555.
3. T. Lu and F. Chen, *Journal of Computational Chemistry*, 2011, **33**, 580-592.